AD-A182 873 A NEW TECHNIQUE FOR THE CHARACTERIZATION OF CESIUM BEAM TUBE PERFORMANCE (U) AEROSPACE CORP EL SEGUNDO CA ELECTRONICS RESEARCH LAB J P HURRELL ET AL 20 JUL 87 1/1

UNCLASSIFIED TR-0086A(2925-08)-1 SD-TR-87-32 F/G 9/1 NL

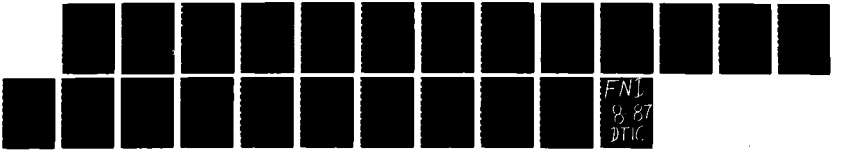

FNL
8 87
DTIC

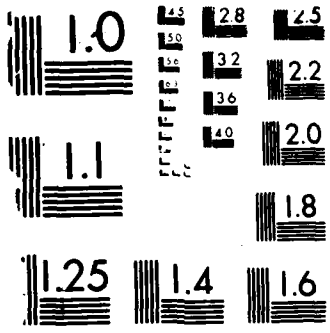

MICROCOPY RESOLUTION TEST CHART

REPORT SD-TR-87-32

A New Technique for the Characterization of Cesium Beam Tube Performance

J. P. HURRELL, W. A. JOHNSON, S. K. KARUZA, and F. J. VOIT
Electronics Research Laboratory
Laboratory Operations
The Aerospace Corporation
El Segundo, CA 90245

20 July 1987

Prepared for

SPACE DIVISION
AIR FORCE SYSTEMS COMMAND
Los Angeles Air Force Station
P.O. Box 92960, Worldway Postal Center
Los Angeles, CA 90009-2960

This report was submitted by The Aerospace Corporation, El Segundo, CA 90245, under Contract No. F04701-85-C-0086-P00016 with the Space Division, P.O. Box 92960, Worldway Postal Center, Los Angeles, CA 90009-2960. It was reviewed and approved for The Aerospace Corporation by M. J. Daugherty, Director, Electronics Research Laboratory.

Lt Michael J. Mitchell/CWNwas the project officer for the Mission-Oriented Investigation and Experimentation (MOIE) Program.

This report has been reviewed by the Public Affairs Office (PAS) and is releasable to the National Technical Information Service (NTIS). At NTIS, it will be available to the general public, including foreign nationals.

This technical report has been reviewed and is approved for publication. Publication of this report does not constitute Air Force approval of the report's findings or conclusions. It is published only for the exchange and stimulation of ideas.

Michael J Mitchell

MICHAEL J. MITCHELL, Lt, USAF
MOIE Project Officer
SD/CWNZS

Joseph Hess

JOSEPH HESS, GM-15
Director, AFSTC West Coast Office
AFSTC/WCO OL-AB

UNCLASSIFIED

SECURITY CLASSIFICATION OF THIS PAGE

AD-A182 813

REPORT DOCUMENTATION PAGE

1a. REPORT SECURITY CLASSIFICATION UNCLASSIFIED	1b. RESTRICTIVE MARKINGS
2a. SECURITY CLASSIFICATION AUTHORITY	3. DISTRIBUTION/AVAILABILITY OF REPORT Approved for public release; distribution unlimited.
2b. DECLASSIFICATION/DOWNGRADING SCHEDULE	
4. PERFORMING ORGANIZATION REPORT NUMBER(S) TR-0086A(2925-08)-1	5. MONITORING ORGANIZATION REPORT NUMBER(S) SD-TR-87-32
6a. NAME OF PERFORMING ORGANIZATION The Aerospace Corporation Laboratory Operations 6b. OFFICE SYMBOL (If applicable)	7a. NAME OF MONITORING ORGANIZATION Space Division
6c. ADDRESS (City, State and ZIP Code) El Segundo, CA 90245	7b. ADDRESS (City, State and ZIP Code) Los Angeles, CA 90009-2960
8a. NAME OF FUNDING/SPONSORING ORGANIZATION Space Division 8b. OFFICE SYMBOL (If applicable) AFSTC/WCO	9. PROCUREMENT INSTRUMENT IDENTIFICATION NUMBER F04701-85-C-0086-P00016
8c. ADDRESS (City, State and ZIP Code) Los Angeles, CA 90009-2960	10. SOURCE OF FUNDING NOS. PROGRAM ELEMENT NO. / PROJECT NO. / TASK NO. / WORK UNIT NO.
11. TITLE (Include Security Classification) A New Technique for the Characterization of Cesium Beam Tube Performance	
12. PERSONAL AUTHOR(S) J. P. Hurrell, W. A. Johnson, S. K. Karuza, F. J. Voit	
13a. TYPE OF REPORT 13b. TIME COVERED FROM _____ TO _____	14. DATE OF REPORT (Yr., Mo., Day) 1987 July 20 15. PAGE COUNT 21
16. SUPPLEMENTARY NOTATION	
17. COSATI CODES FIELD / GROUP / SUB. GR.	18. SUBJECT TERMS (Continue on reverse if necessary and identify by block number) Atomic clocks Cesium beam tubes Electron-multiplier gain and noise

19. ABSTRACT (Continue on reverse if necessary and identify by block number)

Cesium beam tube atomic standards tend to exhibit a decreasing beam tube current with time. This report describes a technique to measure noninvasively the product of electron-multiplier gain and noise figure, as well as tube signal and noise performance, thus providing information to discriminate between possible causes of decreasing beam tube current. The technique characterizes cesium beam tube performance without measuring clock frequency stability. Consequently, no extensive analysis of long-term data is required. The technique is also applicable to a similar evaluation of photomultiplier tubes.

20. DISTRIBUTION/AVAILABILITY OF ABSTRACT UNCLASSIFIED/UNLIMITED ☒ SAME AS RPT. ☐ DTIC USERS ☐	21. ABSTRACT SECURITY CLASSIFICATION Unclassified
22a. NAME OF RESPONSIBLE INDIVIDUAL	22b TELEPHONE NUMBER (Include Area Code) 22c. OFFICE SYMBOL

DD FORM 1473, 83 APR EDITION OF 1 JAN 73 IS OBSOLETE.

UNCLASSIFIED

SECURITY CLASSIFICATION OF THIS PAGE

PREFACE

The authors wish to acknowledge the technical assistance of M. F. Bottjer, W. A. Garber, and D. Y. Watanabe, who contributed in developing the software and hardware for these measurements.

CONTENTS

FIGURES

TABLE

I. INTRODUCTION

Clock performance is determined by the signal-to-noise ratio of the detected cesium (Cs) atomic resonance at 9.2 GHz. If this ratio degrades, the white-noise part of the Allan variance will degrade accordingly. The ratio is ultimately limited by the performance of the beam tube itself. In particular, the Cs atomic beam is detected and amplified before the signal is inserted into the electronic servo system. Not only the beam intensity, but also the noise figure of the detector will determine this ratio. The ratio is more dependent on the performance of the Cs ion detector (first dynode) than on the gain of the rest of the electron multiplier (Fig. 1) (succeeding dynode multiplication), unless the detector's secondary electron emission is severely degraded. Radically reduced emission from the detector is similar to reduced Cs beam flux and degrades the signal-to-noise ratio. With this new proposed measurement system, the output-noise characteristics of the electron multiplier can be studied to determine whether it is possible to separate the loss of first-dynode emission from emission loss at successive dynodes. The loss of output signal by up to an order of magnitude has been observed on some tubes, and is ascribed to multiplier degradation.

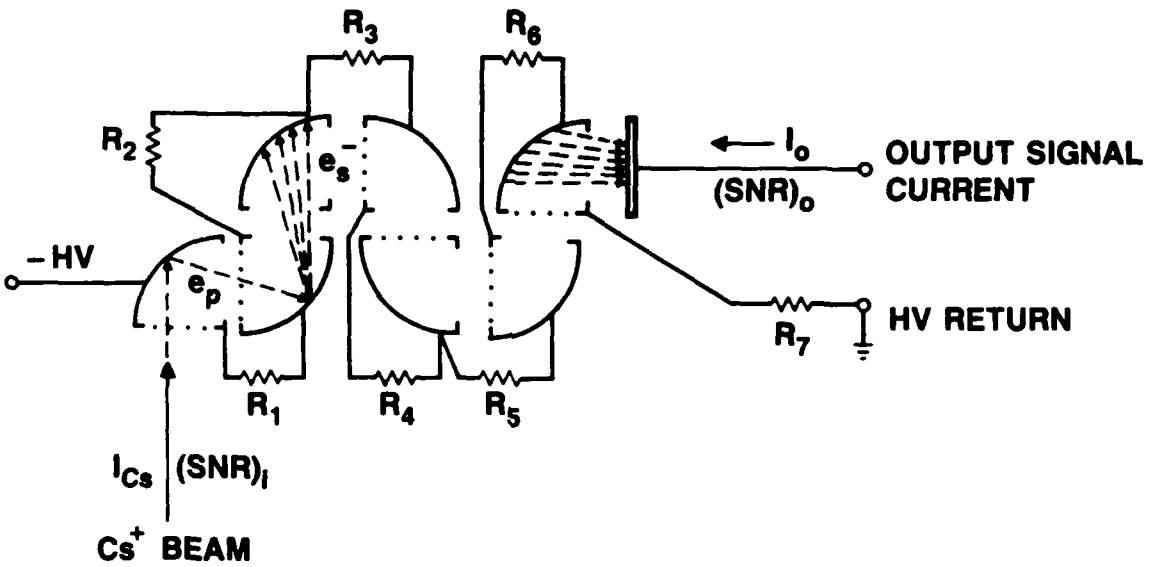

Fig. 1. Cesium Beam Tube Electron Multiplier

II. DISCUSSION

For an average Cs ion current I_{Cs} into the first dynode of the electron multiplier in the Cs beam tube, the noise density $\Phi_i(f)$ of the current will be given[1] by

$$\Phi_i(f) = 2qI_{Cs} \tag{1}$$

where q = charge on an electron = 1.602×10^{-19} Coulomb. Then the signal-to-noise ratio for a 1-Hz noise bandwidth at the first-dynode input is

$$(SNR)_i \equiv \frac{\text{signal power}}{\text{noise power/Hz}} = \frac{(\text{dc signal current})^2}{\Phi_i(f)} = \frac{(I_{Cs})^2}{2q\ I_{Cs}} = \frac{I_{Cs}}{2q} \tag{2}$$

Depending on the conversion efficiency of the first dynode and the gain of the remaining dynodes, the output signal-to-noise ratio of the multiplier will be degraded by some factor F. Then the output signal-to-noise ratio for a 1-Hz noise bandwidth becomes

$$(SNR)_o = \frac{I_{Cs}}{2qF} \tag{3}$$

The conversion efficiency of the first dynode is expected to be about unity, which will result in a degradation factor F of about two. The remaining dynodes will have a much smaller effect on the value of F. Consequently F is expected to be slightly larger than two. If G and I_o are respectively the gain and the current output of the electron multiplier, then

$$I_o = GI_{Cs} \tag{4}$$

Combining (3) and (4) gives

$$FG = \frac{I_o}{2q(SNR)_o} \tag{5}$$

Thus the factor FG can be calculated from measurements of I_o and $(SNR)_o$, and a number of conclusions can be drawn from the measurements of I_o and $(SNR)_o$ and the calculation of FG. Perhaps most important, the measurement of $(SNR)_o$ sets the minimum value that the Allan variance of the clock can have for any given long integration time τ. ("Long" in this usage means that the clock loop gain is very high for frequencies on the order of $1/\tau$.) Some distinctions can also be made between possible effects when I_o, $(SNR)_o$, and FG change. For example, a graceful degradation of electron-multiplier gain (i.e., where the gain of each stage degrades slightly) would result in I_o and FG decreasing proportionately, with $(SNR)_o$ staying essentially constant. If the microwave power into the tube changed, the result would be a proportional change in I_o and $(SNR)_o$, with FG staying constant. Here it is assumed that the initial power setting was for a maximum in I_o. Writing α for the Cs conversion efficiency of the detector surface and δ for the gain of each of the succeeding n dynodes,[1]

$$G = \alpha\delta^n \tag{6}$$

and

$$F = 1 + \frac{1}{\alpha}\left(\frac{\delta}{\delta-1}\right) \text{ (for large n).} \tag{7}$$

It is apparent that a loss in gain through a reduction in either α or δ will affect the product FG differently. If α is reduced from 1 to 0.5, the gain will be reduced by a factor of 0.5, but the product FG will be reduced by a factor of 0.79 (assuming $\delta = 4$). If the gain reduction by a factor of 0.5 is cuased by a reduction in δ, however, the product FG will essentially be reduced by the same factor of 0.5. Consequently, a measurement of FG before and after a loss of beam tube current caused by multiplier degradation will differentiate between first-dynode and later dynode degradation. If the beam current loss is not caused by muliplier degradation, the product FG will remain essentially unchanged.

III. MEASUREMENTS

A block diagram of the measurement system is shown in Fig. 2. The noise bandwidth (NBW) of the 30-Hz bandpass filter was 7.23 Hz. The choice of the 30-Hz measurement frequency is arbitrary, since the noise density out of the tube is independent of frequency as predicted by Eq. (1). This is demonstrated in Fig. 3. Figure 3(a) shows the noise output of the current-to-voltage (I/V) converter when the converter is terminated in an impedance approximately equal to the tube's output impedance. Figure 3(b) shows the noise output of the I/V converter when it is connected to the tube. The microwave power into the beam tube was adjusted for maximum current out of the tube. The tube used for the measurements was a commercial Cs beam tube. A Spectral Dynamic model SD301D spectrum analyzer was used for these measurements. From Fig. 3(b) it is seen that the tube noise density is flat; it is 37 dB above the noise floor of the measurement system, and 30 dB above the spectral spikes of the measurement system. The average current I_o out of the tube is measured by connecting the tube directly to a Keithley model 485 picoammeter. Figure 4 shows the relationship between the input and output power spectral densities of the electron multiplier. The added noise at the output results from the finite gain of the electron-multiplier dynodes, primarily the first dynode. To measure this noise, a bandpass filter must be used to normalize the noise power per hertz.

To illustrate the usefulness of the system, two experiments were performed. In the first, the electron-multiplier voltage was varied from -2000 V to -1375 V. Microwave power and tuning were adjusted for maximum I_o for a multiplier voltage of -2000 V. In the second, the multiplier voltage was held constant at -2000 V and the microwave power level was varied from 0 to 152 μW . The results are shown Figs. 5 and 6. The current-to-voltage gain K from the tube output to the input of the HP 3400 true rms voltmeter was measured to be 2.165×10^9 V/A. Using the measured noise bandwidth of the filter, the $(SNR)_o$ is calculated to be

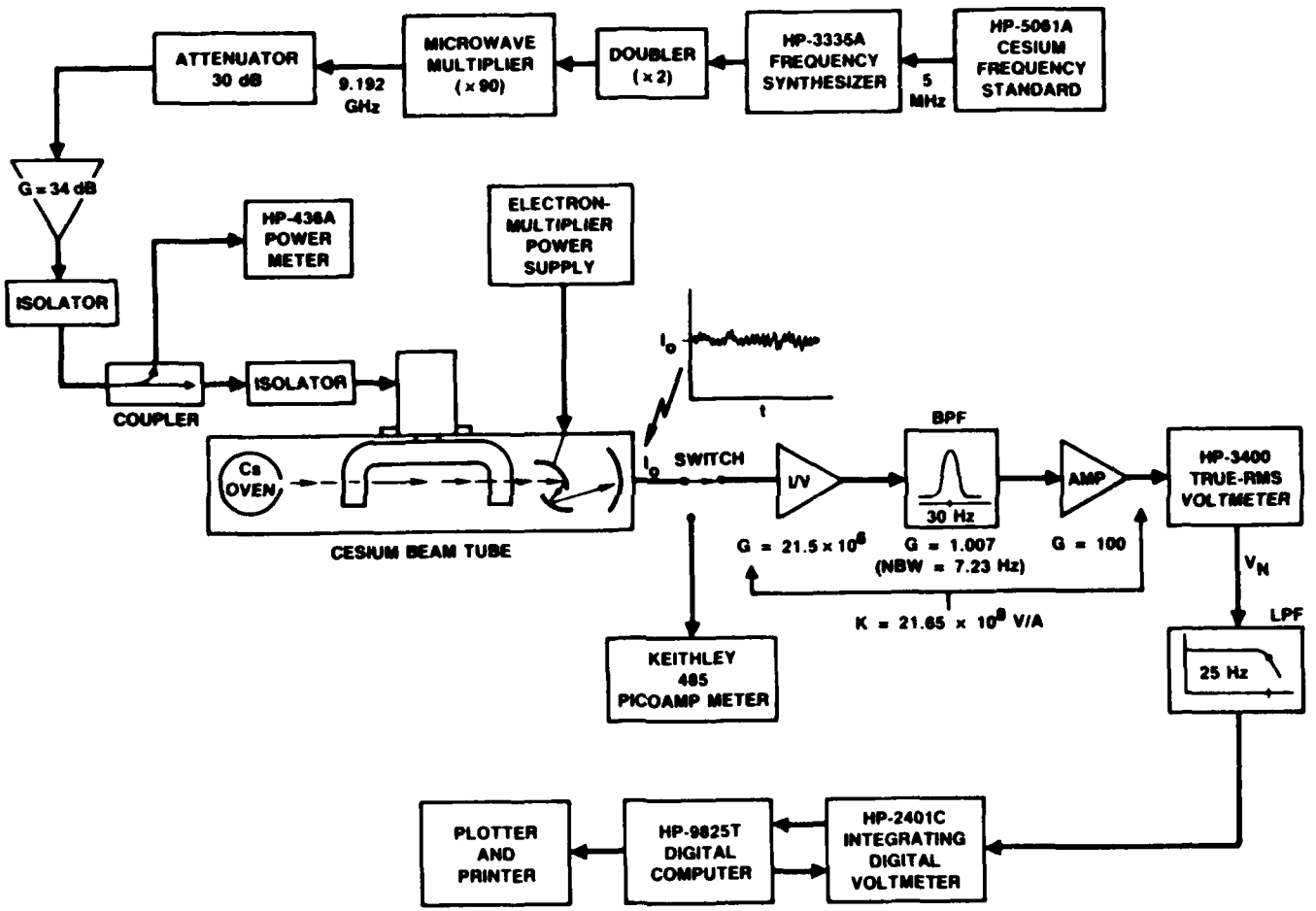

Fig. 2. Block Diagram of Noise Measurement System

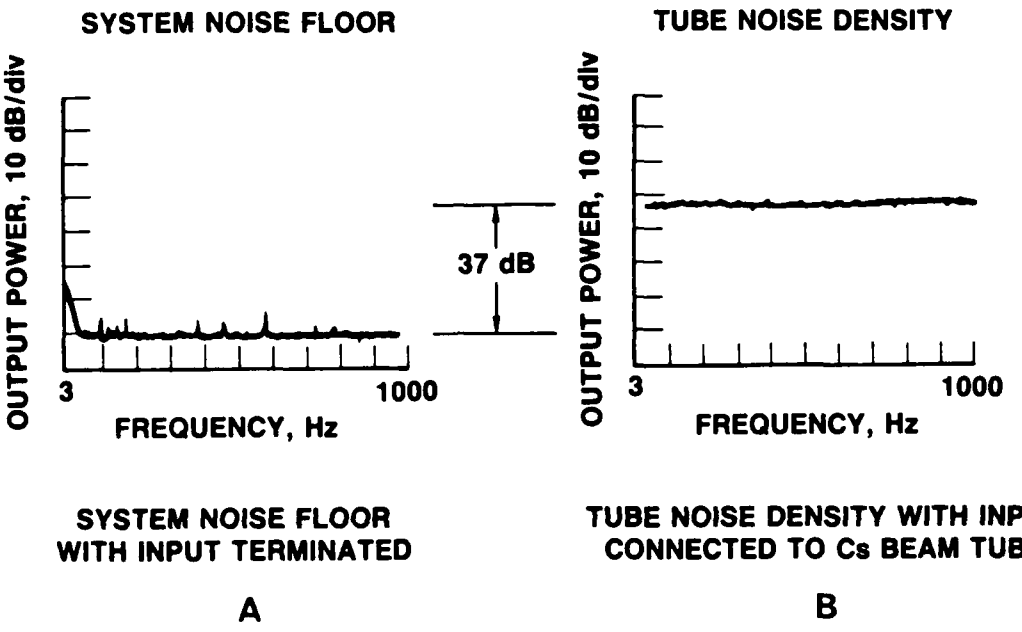

Fig. 3. Power Spectrum of Current-to-Voltage (I/V) Converter Output. (a) System noise floor. (b) Tube noise density.

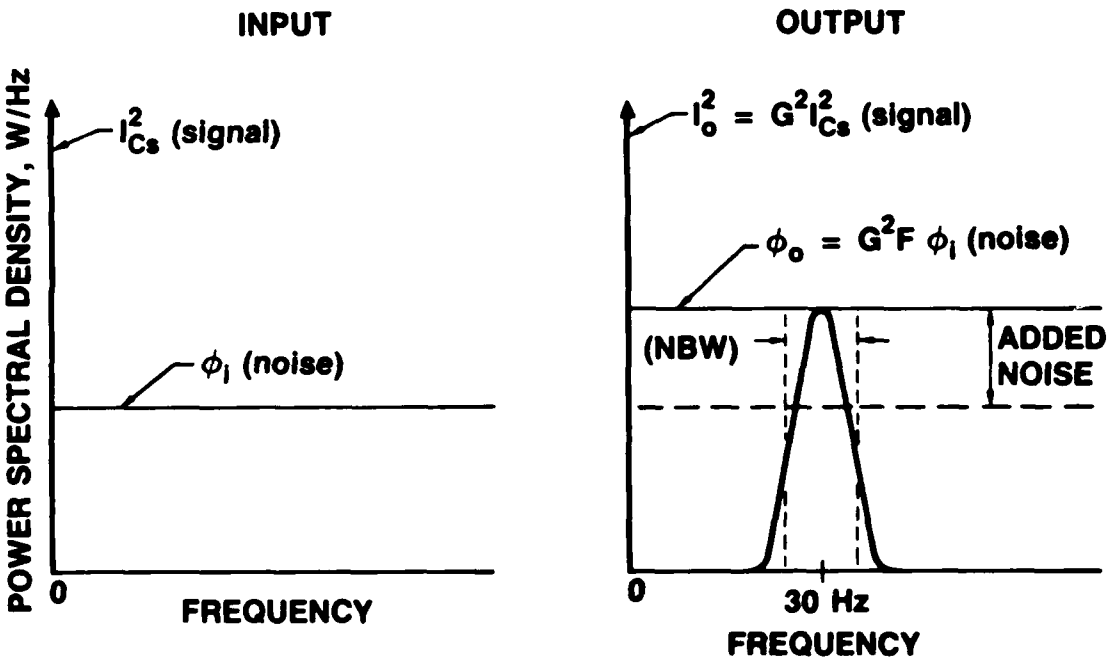

Fig. 4. Power Spectral Density of Electron Multiplier

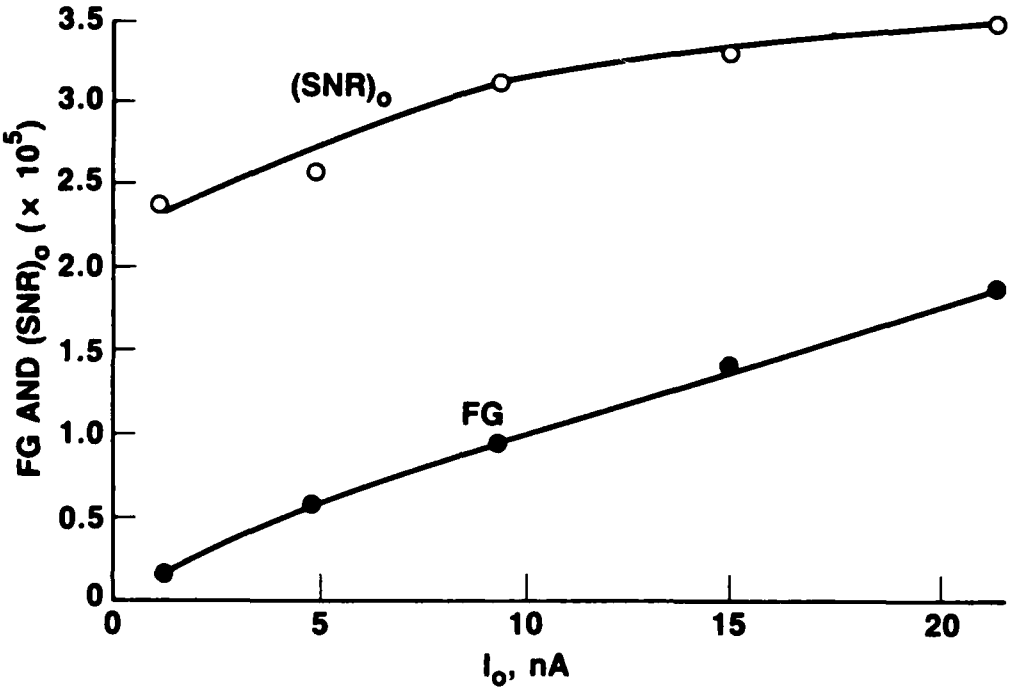

Fig. 5. Relative Gain and Signal-to-Noise Ratio: Electron-Multiplier Voltage Varied

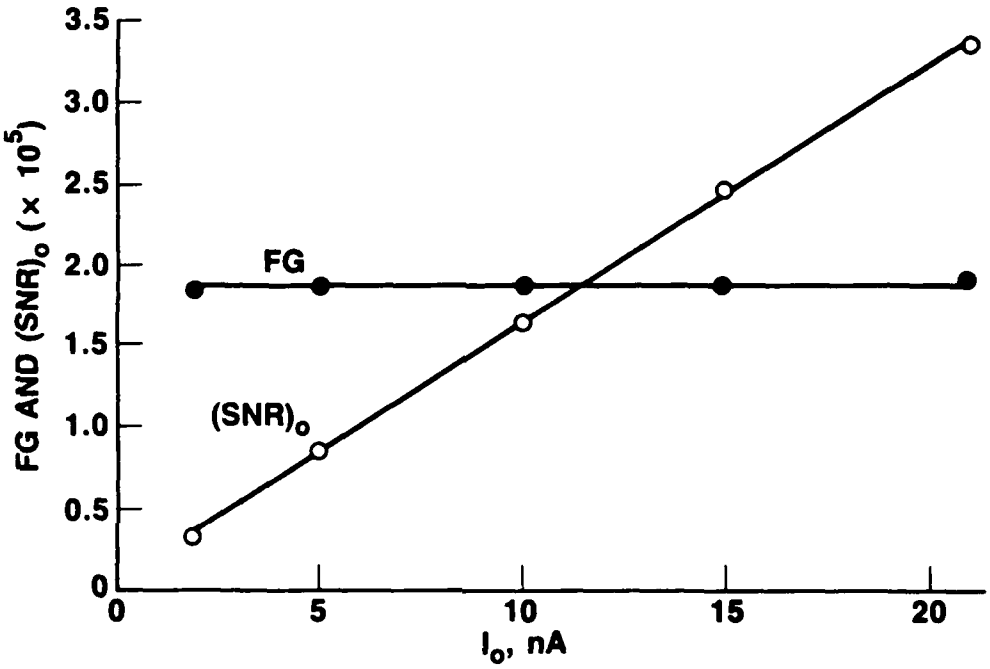

Fig. 6. Relative Gain and Signal-to-Noise Ratio: Microwave Power Varied

$$(SNR)_o = \frac{\text{signal power}}{\text{noise power/Hz}} = \frac{(\text{dc signal current})^2}{(\text{noise current}/\sqrt{NBW})^2}$$

$$= 3.389 \times 10^{19} \left(\frac{I_o^2}{\bar{V}_N}\right) \tag{8}$$

FG can then be computed from Eq. (5) to be

$$FG = 0.0921 \frac{(\bar{V}_N)^2}{I_o} \tag{9}$$

Figure 5 shows that FG is aproximately a linear function of I_o, and that $(SNR)_o$ decreases slightly as I_o decreases. Both of these results are consistent with electron-multipler gain decreasing gracefully with decreasing dynode voltage.

Figure 6 shows that $(SNR)_o$ decreases linearly with I_o and that FG stays essentially constant. Both of these results are consistent with the conclusion that $(SNR)_o$ changes with varying microwave power, as predicted by Eq. (3), while the electron-multiplier performance is unaffected (i.e., FG = constant).

A printout of a typical data output is shown in Table 1. The data set consists of 50 averages, each 10 sec long. Each average is printed out, along with the mean of the data set. A linear least-squares fit to the data set is computed, then the standard deviation about this fit is computed and printed out, along with the slope and y-intercept of the fit. The standard deviation of the mean of the data set is calculated by dividing the standard deviation of the data set by the square root of the number of samples. Thus, for example, the standard deviation of the 0.3358-V mean in the data set would be $0.0123/\sqrt{50} = 1.47$ mV. To determine the noise floor of the measurement system, a similar run was made with the I/V converter terminated in an impedance comparable to that for the beam tube output. With the HP 3400 scale set to 10 mV, the standard deviation of the data set was calculated to be 6.83 mV. This data set also consisted of 50 averages, each 10 sec long. The standard

Table 1. Measurement Data of the Electron Multiplier's Relative Gain and Output Signal-to-Noise Ratio

V_N VALUES (taken with HP-3400 on 300-mV scale)

-0.3297920	-0.3356450	-0.3129540	-0.3559810	-0.3387390	-0.3317080
-0.3462920	-0.3225170	-0.3421480	-0.3372390	-0.3423870	-0.3490170
-0.3268920	-0.3502590	-0.3549790	-0.3369340	-0.3359900	-0.3264090
-0.3385610	-0.3541650	-0.3443630	-0.3526960	-0.3500570	-0.3156810
-0.3259510	-0.3168740	-0.3419060	-0.3240740	-0.3483840	-0.3235480
-0.3225750	-0.3490520	-0.3224680	-0.3489750	-0.3265940	-0.3490910
-0.3487700	-0.3423870	-0.3348590	-0.3162830	-0.3160940	-0.3292870
-0.3290710	-0.3400840	-0.3512980	-0.3155360	-0.3290930	-0.3211600
-0.3410310	-0.3448130				

No. OF POINTS = 50
INTEG TIME (sec) = 10.00000000
MEAN = -0.33581286
STD DEVIATION = 0.01233401
SLOPE = 0.00011999
Y INTERCEPT = -0.33887260

FG = 187304.88
$(SNR)_o$ = 83144.879

deviation of the mean would then be $6.83/\sqrt{50} = 0.966$ mV. Since the HP 3400 outputs 1 V for a full-scale reading, no matter what scale it is set on; this means, for example, that the measurement system noise for the 0.3358-V mean, which resulted from averages taken on the 300-mV scale, would be approximately (300/10) × (335.8/0.966) = 10,494 times below the mean. In other words, the noise floor is about 80 dB below this measurement. The worst noise-floor contribution for all of the data of Figs. 4 and 5 occurred for the last point in Fig. 4. For this point the noise floor was about (30/10) × (488.9/0.966) = 1518 times below the mean. This equates to a noise floor about 64 dB below the measurement. In short, the data are negligibly affected by noise either in the signal itself or inherent in the measurement system.

IV. SUMMARY

A simple technique to determine the signal and noise performance of a Cs beam tube quickly, accurately, and noninvasively has been described. This technique also permits some degree of discrimination between several possible causes of performance degradation in frequency standards. A test setup was designed and constructed to examine the usefulness of the proposed technique. The agreement between the test results and the analytical predictions was found to be excellent. In particular, the product of electron-multiplier gain and its noise figure has been determined.

REFERENCE

1. A. Van der Ziel, Noise in Measurements (New York: Wiley, 1976), p. 139.

LABORATORY OPERATIONS

The Aerospace Corporation functions as an "architect-engineer" for national security projects, specializing in advanced military space systems. Providing research support, the corporation's Laboratory Operations conducts experimental and theoretical investigations that focus on the application of scientific and technical advances to such systems. Vital to the success of these investigations is the technical staff's wide-ranging expertise and its ability to stay current with new developments. This expertise is enhanced by a research program aimed at dealing with the many problems associated with rapidly evolving space systems. Contributing their capabilities to the research effort are these individual laboratories:

Aerophysics Laboratory: Launch vehicle and reentry fluid mechanics, heat transfer and flight dynamics; chemical and electric propulsion, propellant chemistry, chemical dynamics, environmental chemistry, trace detection; spacecraft structural mechanics, contamination, thermal and structural control; high temperature thermomechanics, gas kinetics and radiation; cw and pulsed chemical and excimer laser development including chemical kinetics, spectroscopy, optical resonators, beam control, atmospheric propagation, laser effects and countermeasures.

Chemistry and Physics Laboratory: Atmospheric chemical reactions, atmospheric optics, light scattering, state-specific chemical reactions and radiative signatures of missile plumes, sensor out-of-field-of-view rejection, applied laser spectroscopy, laser chemistry, laser optoelectronics, solar cell physics, battery electrochemistry, space vacuum and radiation effects on materials, lubrication and surface phenomena, thermionic emission, photosensitive materials and detectors, atomic frequency standards, and environmental chemistry.

Computer Science Laboratory: Program verification, program translation, performance-sensitive system design, distributed architectures for spaceborne computers, fault-tolerant computer systems, artificial intelligence, microelectronics applications, communication protocols, and computer security.

Electronics Research Laboratory: Microelectronics, solid-state device physics, compound semiconductors, radiation hardening; electro-optics, quantum electronics, solid-state lasers, optical propagation and communications; microwave semiconductor devices, microwave/millimeter wave measurements, diagnostics and radiometry, microwave/millimeter wave thermionic devices; atomic time and frequency standards; antennas, rf systems, electromagnetic propagation phenomena, space communication systems.

Materials Sciences Laboratory: Development of new materials: metals, alloys, ceramics, polymers and their composites, and new forms of carbon; nondestructive evaluation, component failure analysis and reliability; fracture mechanics and stress corrosion; analysis and evaluation of materials at cryogenic and elevated temperatures as well as in space and enemy-induced environments.

Space Sciences Laboratory: Magnetospheric, auroral and cosmic ray physics, wave-particle interactions, magnetospheric plasma waves; atmospheric and ionospheric physics, density and composition of the upper atmosphere, remote sensing using atmospheric radiation; solar physics, infrared astronomy, infrared signature analysis; effects of solar activity, magnetic storms and nuclear explosions on the earth's atmosphere, ionosphere and magnetosphere; effects of electromagnetic and particulate radiations on space systems; space instrumentation.

END

8-87

DTIC